Titania−Sepiolite Nanocomposites Prepared by a Surfactant Templating Colloidal Route

Pilar Aranda,[†] Robert Kun,[‡] M. Angeles Martín-Luengo,[†] Sadok Letaïef,[†,§] Imre Dékány,[‡,△] and Eduardo Ruiz-Hitzky*,[†]

Instituto de Ciencia de Materiales de Madrid, CSIC, Cantoblanco, E-28049 Madrid, Spain, Supramolecular and Nanostructured Materials Research Group, Hungarian Academy of Sciences, and Department of Colloid Chemistry, University of Szeged, Aradi Vértanuk tere 1, H-6720 Szeged, Hungary

Received August 9, 2007. Revised Manuscript Received October 9, 2007

Microfibrous TiO_2−sepiolite and TiO_2/SiO_2−sepiolite nanocomposites were prepared following a colloidal route based on the controlled hydrolysis of alkoxides in the presence of cetyltrimethylammonium−sepiolite gel. In this way, titanium(IV) isopropoxide and tetramethoxysilane were used as titania and silica precursors, respectively, being incorporated within the organophilic layer developed on the surface of the silicate microfibers and further hydrolyzed in this region. The hydrolysis of the precursor gives highly viscous colloidal systems leading to a spontaneous heterocoagulation process of the colloidal system. Drying and thermal treatments of the resulting gels ensure the elimination of water and organic matter, driving to the formation of TiO_2 nanoparticles homogeneously distributed on the surface of the sepiolite microfibers. The nanocomposites were characterized by chemical analyses, transmission electron microscopy, field emission scanning electron microscopy, X-ray diffraction, thermogravimetric/differential thermal analysis, and N_2 adsorption. They were tested as photocatalysts in the photo-oxidation of phenol in an aqueous medium, showing the efficiency of the anatase containing nanocomposites in the removal of this selected pollutant model molecule. Thiourea was incorporated to increase the TiO_2 anatase phase stability, improving in this manner the photocatalytic activity of the TiO_2−sepiolite nanocomposites. It has been shown that sepiolite has a positive synergistic effect on the TiO_2 photocatalysis.

1. Introduction

The assembly of nanosized species, such as metal clusters and metal−oxide nanoparticles, onto porous solids represents a topic largely studied with the aim to develop improved supported heterogeneous catalysts.[1] In this context, the immobilization of nanoparticles on the inner and outer surfaces of inorganic supports results in the formation of nanocomposite materials which often have high specific surface area and porosity because of their topochemical characteristics. Furthermore, they might be good adsorbent and/or catalytic materials as the synergic effects of the nanoparticle support systems may become relevant.[2] Supports like zeolites,[3] activated carbon,[4,5] and silica[6] are the most widely used solids, together with natural and surface modified clay minerals like montmorillonite, vermiculite, sepiolite, and so forth.[7–9] These nanoparticle-supported materials are of great interest in the study of photocatalytic reactions for the removal of nonfilterable pollutants and dissolved organic compounds from water, which is a frequent problem in sewage treatments. They can also be efficiently used for the removal of dyes,[10–12] halogenated organic compounds,[13,14] and pesticides[15] among other organic pollutants resulting from industrial and agricultural applications.

Among the clay mineral family, the layered silicates belonging to the smectite group are the most common supports applied to perform as this class of materials. However, the access to the internal surface (intracrystalline region) of these solids is hindered except when the nanoparticles act as pillars (pillared clays), which was a topic investigated during the last two decades[16–20] and included

* Corresponding author. E-mail: eduardo@icmm.csic.es.
† CSIC.
‡ Hungarian Academy of Sciences.
§ Present address. Department of Chemistry, University of Ottawa, 10 Marie Curie, Ottawa, Ontario K1N6N5, Canada.
△ University of Szeged.

(1) Thomas, J. M.; Thomas, W. J. *Principles and Practice of Heterogeneous Catalysis*; Wiley-VCH: Weinheim, Germany, 1997.
(2) Zou, L.; Luo, Y.; Hooper, M.; Hu, E. *Chem. Eng. Process.* **2006**, *45*, 959.
(3) Reddy, E. P.; Davydov, L.; Smirniotis, P. *Appl. Catal., B* **2003**, *42*, 1.
(4) Herrmann, J. M.; Matos, J.; Disdier, J.; Guillard, C.; Laine, J.; Malato, S.; Blanco, J. *Catal. Today* **1999**, *54*, 255.
(5) Nagaoka, S.; Hamasaki, Y.; Ishihara, S.-I.; Nagata, M.; Iio, K.; Nagasawa, C.; Ihara, H. *J. Mol. Catal. A* **2002**, *177*, 255.
(6) Chuan, X.-Y.; Hirano, M.; Inagaki, M. *Appl. Catal., B* **2004**, *51*, 255.
(7) Mogyorósi, K.; Dékány, I.; Fendler, J. H. *Langmuir* **2003**, *19*, 2938.
(8) Ding, Z.; Zhu, H. Y.; Greenfield, P. F.; Lu, G. Q. *J. Colloid Interface Sci.* **2001**, *238*, 267.
(9) Yoneyama, H.; Haga, S.; Yamanaka, S. *J. Phys. Chem.* **1989**, *93*, 4833.
(10) Saeed, B.; Bukallah, M. A.; Rauf, S.; Salman, A. *Dyes Pigm.* **2007**, *72*, 353.
(11) Fernández, J.; Kiwi, J.; Baeza, J.; Freer, J.; Lizama, C.; Mansilla, H. D. *Appl. Catal., B* **2004**, *48*, 205.
(12) Bouzaida, I.; Ferronato, C.; Chovelon, J. M.; Rammah, M. E.; Herrmann, J. M. *J. Photochem. Photobiol., A* **2004**, *168*, 23.
(13) Kun, R.; Szekeres, M.; Dékány, I. *Appl. Catal., B* **2006**, *68*, 49.
(14) Calza, P.; Minero, C.; Hiskia, A.; Papaconstantinou, E.; Pelizzetti, E. *Appl. Catal., B* **2001**, *29*, 23.
(15) Muneer, M.; Bahnemann, D. *Appl. Catal., B* **2002**, *36*, 95.
(16) *Pillared Layered Structures. Current Trends and Applications*; Mitchell, I. V. , Ed.; Elsevier: London, 1990.
(17) Pillared Clays (special issue, Burch, R., Ed.) *Catalysis Today* **1988**, *2*, 185.

10.1021/cm702251f CCC: $40.75
Published on Web 12/14/2007

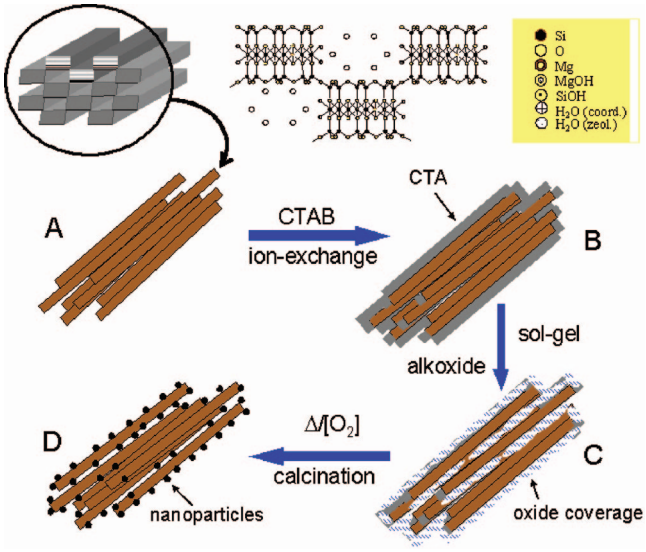

Figure 1. Schematic representation of the procedure leading to TiO_2−sepiolite nanocomposites by the reaction of TIPOTI with controlled amounts of water at the CTA−sepiolite interphase and further calcinations to promote the TiO_2 nanoparticles formation.

titania-pillared clays.[21] Recently, other alternatives imply that clay delamination leads to delaminated clays incorporating silica or titania.[22–24]

In the present work, we have developed new inorganic–inorganic nanocomposites based on sepiolite associated to titanium dioxide nanoparticles. Sepiolite is a nonlayered clay mineral showing a microfibrous morphology and a particular texture that provides a high specific surface area (>300 m^2/g) and porous volume (~0.4 cm^3/g). Therefore, this silicate appears as an attractive support, scarcely studied to the present, for the assembly of small-size metals and metal−oxide aggregates (clusters and nanoparticles) that have been mainly employed for catalytic purposes.[25–28] This clay mineral is a hydrated magnesium silicate with the theoretical half-unit-cell formula $Si_{12}O_{30}Mg_8(OH,F)_4(OH_2)_4 \cdot 8H_2O$[29,30] structurally built up by blocks formed by an octahedral sheet of magnesium oxide/hydroxide packed between two tetrahedral silica layers (Figure 1). The periodic inversion of the SiO_4 tetrahedra determines a regular discontinuity of the sheets, which is the origin of the structural cavities (*tunnels*) extended along the *c* axis, that is, the axis of the microfibers,[29] and the presence of silanol groups (Si-OH).[31,32] Those groups can react with organochlorosilanes and alkoxides giving covalently bonded organic–inorganic derivatives,[33–36] which could be useful for anchoring metal−oxide nanoparticles on the sepiolite surface. In this way, we have tried to develop titanium dioxide nanoparticles by reaction of titanium alkoxides with sepiolite in an organophilic environment created at the silicate−reagent interphase. Such environment is assured by cationic surfactants that are easily associated with the silicate surface by ion-exchange reactions with alkylammonium salts solutions.[37]

TiO_2 is one of the most frequently investigated photocatalysts because of its low cost, reduced toxicity, and high chemical stability.[38] Many different ways have been used by different authors to prepare nanosized photocatalytically active TiO_2 particles using either inorganic or organic precursors.[39] The most commonly used method is the sol–gel technique[40,41] in which an organic precursor of titania is first hydrolyzed and the nanoparticles are formed after addition of peptizing agents and/or heating. In many cases, the above mentioned procedure is combined with hydrothermal treatments leading to more porous and better crystallized TiO_2 nanoparticles.[42,43] Another way to increase crystallinity in titanium dioxide nanoparticles from the initially amorphous products consists of calcination processes carried out at high temperature, although this procedure also induces the growth of crystallites.[44] The crystallite size and crystallinity are crucial for the photocatalytic activity of the nanoparticles as UV photons with sufficient energy must interact with them.[45–47] Doping of TiO_2 with transition metals[48] or dye sensitization[49] are common techniques to modify the light absorption properties of this oxide and to enhance its photoefficiency and photoactivity in the visible light region.

(18) Yang, R. T.; Baksh, M. S. A. *AIChE J.* **1991**, *37*, 679.
(19) Ohtsuka, K. *Chem. Mater.* **1997**, *9*, 2039.
(20) Lambert, J. F.; Poncelet, G. *Top. Catal.* **1997**, *4*, 43.
(21) Ooka, C.; Akita, S.; Ohashi, Y.; Horiuchi, T.; Suzuki, K.; Yoshida, H.; Hattori, T. J. *Mater. Chem.* **1999**, *9*, 2943.
(22) Letaïef, S.; Ruiz-Hitzky, E. *Chem. Commun.* **2003**, *24*, 2996.
(23) Letaïef, S.; Martín-Luengo, M. A.; Aranda, P.; Ruiz-Hitzky, E. *Adv. Funct. Mater.* **2006**, *16*, 401.
(24) Yoda, S.; Sakurai, Y.; Endo, A.; Miyata, T.; Otake, K.; Yanagishita, H.; Tsuchiya, T. *Chem. Commun.* **2002**, *14*, 1526.
(25) Barrios-Neira, J.; Rodrique, L.; Ruiz-Hitzky, E. *J. Microsc. Spectrosc. Electron.* **1974**, *20*, 295.
(26) Barrios, J.; Poncelet, G.; Fripiat, J. J. *J. Catal.* **1981**, *63*, 362.
(27) Casal, B.; Bergaya, F.; Challal, D.; Fripiat, J. J.; Ruiz-Hitzky, E.; Van Damme, H. *J. Mol. Catal.* **1985**, *33*, 83.
(28) Güngör, N.; Isci, S.; Günister, E.; Mista, W.; Teterycz, H.; Klimkiewicz, R. *Appl. Clay Sci.* **2006**, *32*, 291.
(29) Brauner, K.; Preisinger, A. *Mineral. Petrogr. Mitt.* **1956**, *6*, 120.
(30) Santarén, J.; Sanz, J.; Ruiz-Hitzky, E. *Clay Miner.* **1990**, *38*, 63.
(31) Ahlrichs, J. L.; Serna, J. C.; Serratosa, J. M. *Clays Clay Miner.* **1975**, *23*, 119.
(32) Ruiz-Hitzky, E. *J. Mater. Chem.* **2001**, *11*, 86.
(33) Ruiz-Hitzky, E.; Fripiat, J. J. *Clays Clay Miner.* **1976**, *24*, 25.
(34) Van Meerbeek, A.; Ruiz-Hitzky, E. *Colloid Polym. Sci.* **1979**, *257*, 178.
(35) Ruiz-Hitzky, E.; Van Meerbeeck, A. In *Handbook of Clay Science*; Bergaya, F., Theng, B. K. G., Lagaly, G., Eds.; Elsevier: London, 2006; Chapter 10.3, p 583.
(36) Gómez-Avilés, A.; Darder, M.; Aranda, P.; Ruiz-Hitzky, E. *Angew. Chem., Int. Ed.* **2007**, *46*, 923.
(37) Alvarez, A.; Santaren, J.; Perez-Castell, R.; Casal, B.; Ruiz-Hitzky, E., Levitz, P.; Fripiat, J. J. In *Proceedings of the International Clay Conference*, Denver, 1985; Schultz, L.G., van Olphen, H., Mumpton, F.A., Eds.; The Clay Minerals Society: Bloomington, 1987; p 370.
(38) Fujishima, A.; Rao, T. N.; Tryk, D. A. *J. Photochem. Photobiol., C* **2000**, *1*, 1.
(39) Khalil, K. M. S.; Baird, T.; Zaki, M. I.; El-Samahy, A. A.; Awad, A. M. *Colloids Surf., A* **1998**, *132*, 31.
(40) Wang, C. C.; Ying, J. Y. *Chem. Mater.* **1999**, *11*, 3113.
(41) Kun, R.; Mogyorósi, K.; Dékány, I. *Appl. Clay Sci.* **2006**, *32*, 99.
(42) Kolenko, Y. V.; Churagulov, B. R.; Kunst, M.; Mazerolles, L.; Colbeau-Justin, C. *Appl. Catal., B* **2004**, *54*, 51.
(43) Yanagisawa, K.; Ovenstone, J. *J. Phys. Chem. B* **1999**, *103*, 7781.
(44) Nishimoto, S.; Ohtani, B.; Kajiwara, H.; Kagiya, T. *J. Chem. Soc., Faraday Trans. 1* **1985**, *81*, 61.
(45) Sakthivel, S.; Hidalgo, M. C.; Bahnemann, D. W.; Geissen, S.-U.; Murugesan, V.; Vogelpohl, A. *Appl. Catal., B* **2006**, *63*, 31.
(46) Calza, P.; Pelizzetti, E.; Mogyorósi, K.; Kun, R.; Dékány, I. *Appl. Catal., B* **2007**, *72*, 314.
(47) Ohtani, B.; Ogawa, Y.; Nishimoto, S.-I. *J. Phys. Chem. B* **1997**, *101*, 3746.
(48) Wang, J.; Uma, S.; Klabunde, K. J. *Appl. Catal., B* **2004**, *48*, 151.
(49) Moona, J.; Yun, C. Y.; Chung, K.-W.; Kang, M.-S.; Yi, J. *Catal. Today* **2003**, *87*, 77.

Doping by nonmetal elements such as carbon,[50] nitrogen,[51] and sulfur[52] has also been investigated. Sulfur doping, which shifts the absorption edge of TiO_2 to a lower energy, appears as an interesting alternative as the S-doped catalyst improves its photocatalytic degradation of organic dyes under visible light irradiation.[53,54]

In the present work, organically modified microfibrous sepiolite was used as the support for nanosized TiO_2 formed by an in situ hydrolysis process between the alkoxide precursor and the surface of the silicate (Figure 1). It is assumed that the organophilic interphase, assured by a surfactant coating, acts like a templating medium which provides titanium dioxide nanoparticles with relatively monodiperse particle sizes on the surface. The initially amorphous titania phase was crystallized by calcination at 500 °C for several hours in air while the surfactant, as the templating agent, was partially burned out and carbonized. TiO_2-SiO_2/sepiolite nanocomposites were also prepared following this colloidal route. This new procedure leads to materials where the TiO_2 phase can be sulfur-doped by using thiourea. The inclusion of sulfur atoms in titanium dioxide is carried out with the aim to increase the stability of the anatase phase and to decrease the excitation band gap energy. The titanium dioxide/sepiolite nanocomposites were tested in photocatalytic experiments using phenol as the pollutant model molecule, proving that these materials can be used as adsorbents/photocatalysts for environmental applications.

2. Experimental Section

Materials. Natural mineral containing >95% of pure sepiolite from the Vallecas-Vicálvaro clay deposits (Madrid, Spain) and commercialized as Pangel S-9 was provided by TOLSA S.A. Hexadecyltrimethylammonium bromide (CTAB, purum, Aldrich) was used in the preparation of the cetyltrimethylammonium (CTA)−sepiolite organoclay derivate. Doubly distilled water (R > 18 MΩ cm) and isopropanol (Fluka, ≥99.8) were used as solvents or reactants. Titanium(IV) isopropoxide (TIPOTI, purum, Fluka) and tetramethoxysilane (TMOS, ≥98%, Fluka) were used as titania and silica precursors, respectively. Thiourea (Reanal, puriss) was employed as reagent for the preparation of sulfur-doped TiO_2 derivatives. Phenol (Aldrich, analytical grade) was tested as model pollutant in the photocatalysis experiments.

Sample Preparation. CTA−sepiolite was prepared by an ion-exchange reaction of sepiolite suspended in water with a calculated amount of CTAB dissolved in water to reach 3 times the cation exchange capacity of the clay mineral (ca. 15 mequiv/100 g) and a final concentration of 2% (grams of sepiolite/100 mL of water). The suspension was stirred for 2 days at 50 °C and then centrifuged, washed three times with water, and dried at 40 °C. From the dried CTA−sepiolite product was prepared a 10% (w/w) homogeneous suspension in isopropanol by using a high speed stirrer (LOMI, Spain); the suspension was stored in polypropylene plastic flasks until usage.

In a first set of experiments, TiO_2−sepiolite nanocomposites were prepared by addition to 10 g of CTA−sepiolite/isopropanol suspension of the required amount of a 50% (v/v) of a TIPOTI/isopropanol mixture to reach final 1:1, 2:1, and 3:1 TIPOTI/CTA−sepiolite ratios. After 5 min of stirring, a calculated amount of water was added dropwise to the suspension. The spontaneous gel formation at room temperature (~22 °C) took between 1 and 30 min depending on the amount of water that was added to the suspension. Prior to calcination, the gel was dried at 40 °C in atmospheric air for 2 days, and finally, the dried samples were calcined at 500 °C for 1 h in an N_2 atmosphere and then in an air flux for an additional 5 h.

Sulfur-doped samples (S-doped TiO_2) were prepared from thiourea that was dissolved in absolute ethanol at 50 °C and cooled to room temperature. To this homogeneous solution was added a calculated amount of TIPOTI dropwise under vigorous stirring at room temperature. The final molar ratio of ethanol/TIPOTI was 50:1, and the ratio of thiourea/TIPOTI was 4:1. Afterward, a calculated amount of water was added dropwise to the ethanol/TIPOTI/thiourea mixture under vigorous stirring. A white precipitate was obtained immediately after the addition of the water. The precipitate was filtered and dried at room temperature. For comparison, pure TiO_2 was precipitated without using thiourea. The samples were calcined at variable temperature in air.

To prepare S-doped TiO_2/sepiolite nanocomposites, a given amount of the CTAB−sepiolite/isopropanol suspension was dropwise mixed with a calculated amount of thiourea dissolved in absolute ethanol. After homogenization of the mixture, variable amounts of the TIPOTI were injected into the stirred suspension. The organoclay/TIPOTI weight ratios were 1:2, 1:3, and 1:4, and the thiourea/TIPOTI molar ratio was 4:1. After slow addition of water to the slurry, the mixture became more viscous because of the hydrolysis and the polycondensation of the titania precursor. The product was dried at 40 °C in atmospheric air and calcined at a variable temperature in an air flux (50 mL/min) during 4−6 h.

The preparation of the TiO_2/SiO_2/CTAB−sepiolite samples was similar to the previous synthesis of S-doped nanocomposites (S−TiO_2/sepiolite), using TIPOTI and TMOS as precursor alkoxides mixed at different ratios (6:4:5 and 2:6:1 of CTA−sepiolite/TIPOTI/TMOS). In this case, the spontaneous gel formation occurs after 1 h of the addition of water. The gel products were air dried at 40 °C before calcinations at 500 °C for 6 h under an air flux (50 mL/min).

Characterization Techniques. C, H, N, and S elemental analysis was performed in a LECO CHNS-932 analyzer. X-ray diffraction (XRD) patterns were obtained in a D8 powder diffractometer (Bruker) using Cu Kα radiation. Fourier transform infrared (FTIR) spectra in the reflectance mode were obtained from samples prepared as pellets (without KBr) using a Bruker ISS 66V-S spectrophotometer. Thermogravimetric and differential thermal analyses were simultaneously recorded on SEIKO SSC/5200 equipment. Samples were examined by scanning electron microscopy (SEM, Zeiss DSM 960), field emission scanning electron microscopy (FE-SEM, FEI Nova NanoSEM 230 and Zeiss Supra VP55), and transmission electron microscopy (TEM, LEO-910 microscope operating at 80 kV) techniques, and in some cases, they were in situ analyzed with an EDX Tacor-Northen Serie Z-II spectrometer or an EDAX 9100 analyzer.

The textural properties of the solids were measured in a Micromeritics ASAP 2010 apparatus with N_2 at 77 K. The samples were outgassed for 16 h at 200 °C to remove any loosely held adsorbed species. The apparent specific surface area (S_{BET}) was obtained by the Brunauer−Emmet−Teller (BET) method, and the external area (S_{ext}) and the micropore volume (V_{mic}) were obtained

(50) Sakthivel, S.; Kisch, H. *Angew. Chem., Int. Ed.* **2003**, *42*, 4908.
(51) Goles, J. L.; Stout, J. D.; Burda, C.; Lou, Y.; Chen, X. *J. Phys. Chem. B* **2004**, *108*, 1230.
(52) Ohno, T.; Mitsui, T.; Matsumura, M. *Chem. Lett.* **2003**, *32*, 364.
(53) Umebayashi, T.; Yamaki, T.; Tanala, S.; Asai, K. *Chem. Lett.* **2003**, *32*, 330.
(54) Ohno, T.; Akiyoshi, M.; Umebayashi, T.; Asai, K.; Mitsui, T.; Matsumura, M. *Appl. Catal., A* **2004**, *265*, 115.

with the *t*-plot method.[55,56] The total pore volume of the micropores and mesopores was calculated from the amount adsorbed at a relative pressure of $p/p^0 = 0.96$, on the desorption branch, equivalent to the filling of all pores below 50 nm diameter. The mesopore size distribution was obtained from the data of the desorption branch assuming slit-shaped pores based on the method of Barrett, Joyner, and Hallender[55] and taking the thickness of the adsorbed layer at each relative pressure from the classical equation of Harkins−Jura.

Photocatalytic Activity Studies. The photocatalysis experiments were carried out in a batch type reactor equipped with an immersion type high pressure Hg arc lamp (150 W, $\lambda = 280$–600 nm). The schematic diagram of the reactor is shown in Figure 1S in the Supporting Information. During the irradiation, thermostatic conditions were applied ($T = 298$ K). Prior to irradiation, 375 mL of the suspension containing the model pollutant (phenol, $c_{init} = 0.5$ mmol/L) and the catalyst material were introduced into the reactor. The adsorption equilibrium was established after 1 h in dark conditions, and afterwards, the light source was switched on. At given time intervals during the illumination, 2 mL portions of the suspension were taken out and further analyzed. The total irradiation time was 2 h in each experiment. The photodegradation of phenol was monitored by a Euroglas TOC-1200 total organic carbon (TOC) analyzer. The samples which contained organic substances (solutions or suspensions) were burned at 1000 °C in the oven of the analyzer in an oxygen atmosphere; an integrated IR detector measured the amount of the formed CO_2, which is proportional to the carbon content of the sample. High purity argon gas was used as the carrier gas in the analyzer. Prior to the analyses, the suspensions were centrifuged and filtered through 0.22 μm hydrophilic PTFE membranes (Millipore Millex).

3. Results and Discussion

The preparation of the TiO_2−sepiolite nanostructured materials consists of the slow hydrolysis and polycondensation reactions of TIPOTI at the organophilic region of a surfactant-modified sepiolite in an isopropanol colloidal suspension. It is well known that sepiolite is able to exchange its metal ions, compensating negative surface charge by long chain alkylammonium cations, such as CTA^+ species.[37] Figure 1 schematically shows the formation of the titanium dioxide precursor, formed at the CTA−sepiolite interphase, by reaction of the TIPOTI molecules located at the organophilic region of the organoclay with controlled amounts of the water molecules that are incorporated into the reaction mixture. As with similar reactions carried out with silicon alkoxides in the interlayer space of organoclays derived from smectites,[22,23] the most salient feature of these processes is the spontaneous gelation that takes place in these colloidal systems. In the present case, the hydrolysis and polycondensation reactions of the titanium alkoxide may occur at room temperature (ca. 22 °C) between 1 and 30 min depending on the amount of water added to the suspension. We have observed that when the TIPOTI/H_2O molar ratio was 1:1, then the gelation time was around 30 min, whereas when the water content (molar ratio = 1:2 or 1:3) was increased, the gelation time strongly decreased until it was around 1–2 min. It must be considered that each $Ti(iPrO)_4$ molecule contains four isopropyl groups, so the stoichiometric molar amount of the water must be multiplied by four in the initial hydrolysis step.

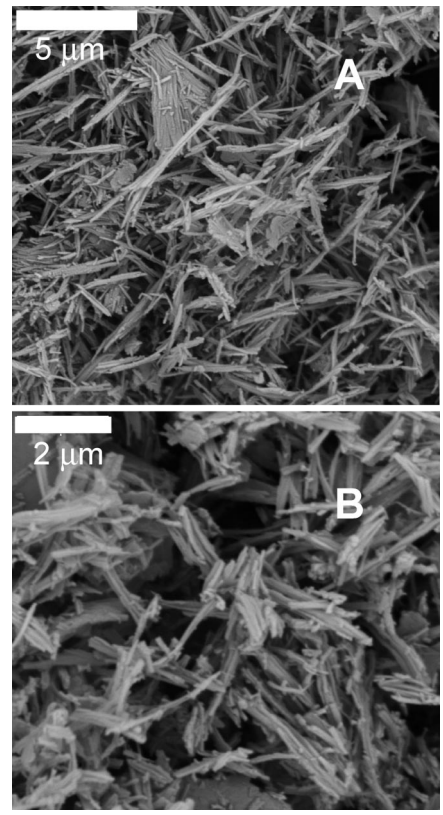

Figure 2. SEM images of S−TiO_2−sepiolite nanocomposites prepared from CTA−sepiolite/thiourea−TIPOTI 1:3 mixtures before (A) and after (B) calcination 600 °C for 4 h in air flux.

To transform the titanium dioxide precursor in anatase nanoparticles, it is required to remove the organic matter (surfactant and remaining isopropoxy groups) by calcination. The conventional procedure applied to mesoporous silica synthesis has been adopted here in the first approach. The dried samples containing the TiO_2 precursor were calcined at 500 °C for 1 h in an N_2 atmosphere and then in air flux (50 mL/min) for 5 h. In these conditions, the formation of nanoparticles of anatase is evidenced by XRD and consists of agglomerated material that completely wraps the sepiolite microfibers, as shown in the SEM images comparing the samples before and after calcination (Figure 2). These materials appear as a black powder indicating that the calcination of the surfactant leads to carbon formation in a collateral process. Although its content is low (∼1% C), the nanostructuration of carbon may contribute to enhance the specific surface area but, as discussed below, the photoactivity of the materials could be unfavorable. We have observed that an increase of the calcination time to remove carbon from the samples is accompanied by the presence of a rutile phase together with the anatase nanoparticles.

It is known that the incorporation of S atoms in the crystal lattice of TiO_2 prevents the phase transition from anatase to rutile during the heat treatments until 400–500 °C.[54] We have observed from XRD patterns that xerogel samples formed from TIPOTI contain a mixture of the anatase and rutile

(55) Rouquerol, F.; Rouquerol, J.; Sing, K. *Adsorption by Powders and Porous Solids-Principles, Methodology and Applications*; Academic Press: London, 1998.
(56) Lippens, B. C.; de Boer, J. H. *J. Catal.* **1965**, *4*, 319.

Table 1. Content in C, H, N, and S Determined by Elemental Chemical Analysis in Various TiO_2−Sepiolite Samples Prepared in This Work

sample starting composition	calcination conditions	C %	S %	N %	H %
CTA−sepiolite	uncalcined	9.7		0.5	2.7
CTA−sepiolite/TIPOTI 1:1	500 °C, 1 h N_2, 5 h air	0.5		0.1	1.0
CTA−sepiolite/TIPOTI 1:2	500 °C, 1 h N_2, 5 h air	0.3		0.0	0.8
CTA−sepiolite/thiourea−TIPOTI[a] 1:2	500 °C, 6 h air	0.5	1.6	0.3	1.5
CTA−sepiolite/thiourea−TIPOTI[a] 1:3	uncalcined	11.8	25.4	22.4	4.0
	500 °C, 4 h air	1.1	1.3	0.3	1.3
	500 °C, 6 h air	1.0	1.5	0.3	1.4
	550 °C, 6 h air	0.8	1.5	0.2	1.2
	600 °C, 4 h air	0.3	1.3	0.1	1.0
CTA−sepiolite/thiourea−TIPOTI[a] 1:4	500 °C, 6 h air	0.4	1.8	0.2	1.3
CTA−sepiolite/thiourea−TIPOTI[a]/TMOS 2:6:1	500 °C, 6 h air	0.3	1.4	0.2	1.1
CTA−sepiolite/thiourea−TIPOTI[a]/TMOS 6:4:5	500 °C, 6 h air	0.9	0.6	0.4	1.6
thiourea/TIPOTI 4:1 xerogel	400 °C, 4 h air	0.4	1.0	0.4	0.1

[a] Reaction mixture incorporating a 4:1 thiourea/TIPOTI ratio.

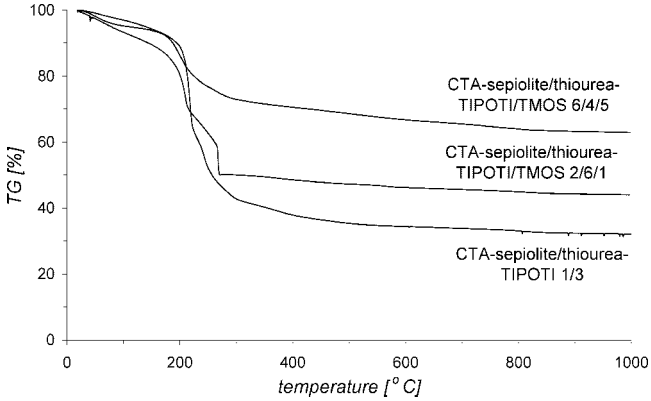

Figure 3. Thermogravimetric curves of several uncalcined sepiolite/TiO_2 nanocomposite intermediate materials.

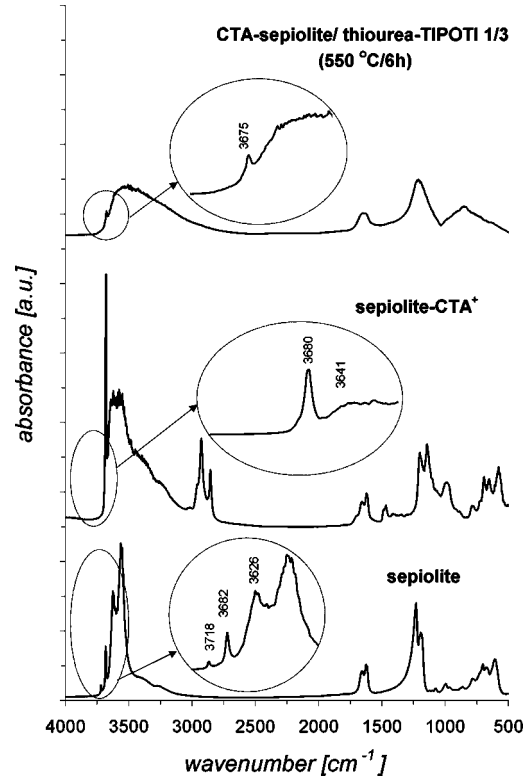

Figure 4. FTIR spectra of (a) sepiolite, (b) CTA−sepiolite, and (c) S-doped TiO_2/sepiolite nanocomposites from a CTA−sepiolite/TIPOTI 1:3 ratio calcined at 550 °C for 6 h.

phases after the treatment at 600 °C (4 h, air atmosphere) whereas the incorporation of thiourea in the xerogel stabilizes the anatase phase (see Figure 2S in the Supporting Information). In this way, we have prepared S-doped samples using thiourea, which is incorporated in the starting mixture together with the titanium isopropoxide, reaching a thiourea/TIPOTI ratio of 4:1 as indicated in the Experimental Section. The resulting nanocomposites were dried and then calcined at different temperatures to optimize the anatase phase formation as well as to avoid the carbon formation. We have observed that by increasing the temperature and the duration of the calcination process, the carbon content of the samples gradually decreases, as monitored by elemental analyses (Table 1). From thermal analysis curves (Figure 3), it can be deduced that it is necessary to heat samples up to 400 °C to remove all of the organic matter. In this context, the calcination products were studied by different techniques to evaluate the elimination of the organic matter, the anatase phase formation, and the collapse of the sepiolite. Thermal treatment at 500 °C for 4–6 h in air atmosphere appears to be the optimal condition to reach the minimization in carbon content, assuring the amorphous−crystalline anatase phase transition without significant structural collapse of the clay mineral according to the FTIR (Figure 4) and XRD (Figure 5) analysis. The bands ascribed to the presence of the surfactant (CTA groups), appearing in the 2800–3000 and 1500–1200 cm^{-1} regions in the IR spectra (Figure 4b) and assigned to the stretching and deformation vibrations of the $-CH_2-$ and CH_3- groups belonging to the alkyl chain, disappear after thermal treatment (Figure 4c), which shows the complete elimination of the surfactant in agreement with elemental analyses (Table 1). XRD patterns of S-doped TiO_2−sepiolite materials calcined 4 h at 500 and 600 °C clearly show the stabilization of the anatase phase (typical diffraction peak at 25.5° (2θ)). The folding of the sepiolite structure at temperatures above 500 °C determines that the characteristic peaks of the sepiolite (e.g., 7.7° (2θ)) disappear for samples treated at higher temperatures (Figure 5).

The above mentioned experimental conditions also guarantee adequate textural characteristics of the resulting nanocomposites (Table 2). The N_2 adsorption isotherms obtained for the S-doped samples calcined at 500, 550, and 600 °C (Figure 6) are of type I/II with hysteresis loops of type H3 according to the IUPAC classification.[55] The precursor sample, that is, the sample dried at 40 °C, shows a type II isotherm with an almost non-existent hysteresis loop and a

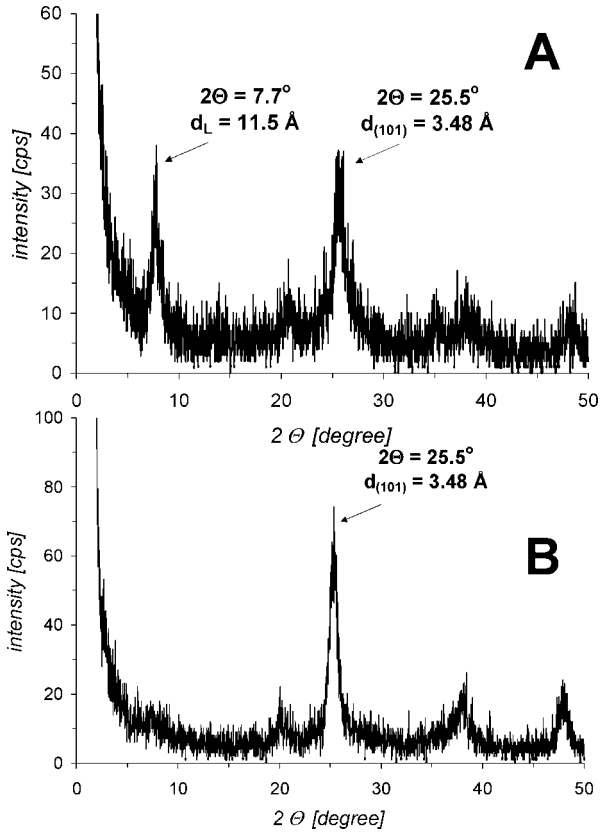

Figure 5. XRD pattern of S−TiO_2/sepiolite nanocomposites prepared from a CTA−sepiolite/TIPOTI 1:3 ratio after calcinations in air during 4 h at (A) 500 °C and (B) 600 °C.

total surface area of 35 m^2/g (of which more than 25 m^2/g is external surface area), a total pore volume close to 0.05 cm^3/g, and a micropore volume of approximately 0.004 cm^3/g. This parent solid has been calcined at three different temperatures as follows: 500 (4 h or 6 h), 550 (4 h), and 600 °C (4 h). The solids with higher total and external surface areas and total pore volumes are those calcined at 500 °C, with the one calcined for 6 h at 500 °C reaching 124 m^2/g, 98 m^2/g, and 0.148 cm^3/g, respectively, for those properties (Table 2).

TEM images show that the uncalcined samples present sepiolite fibers cemented by the gel precursor. When heated, this material evolves leading to the formation of S-doped TiO_2 nanoparticles whose size and distribution are quite similar, independent of the adopted calcination conditions. In contrast to the non-S-doped samples, the size distribution of particles is very homogeneous, being in the 4–8 nm range. Figure 7B shows an example of how those TiO_2 nanoparticles are homogeneously distributed on the sepiolite surface of the nanocomposites compared with the texture of the starting CTA−sepiolite microfibers (Figure 7A). This texture, showing a homogeneous distribution of the TiO_2 nanoparticles, is truly corroborated from the FE-SEM images (Figure 7C) and in the negative picture of the TEM image (inset in Figure 7B). Figure 3S in the Supporting Information also shows FE-SEM and TEM images of uncalcined and calcined nanocomposites prepared in different conditions as additional support on the morphology and disposition of TiO_2 nanoparticles on the sepiolite surface. In that figure, we have also introduced images of the untreated sepiolite fibers for comparative purposes, showing their clean and smooth mineral surfaces.

On the other hand, the stretching O−H vibrations of silanol groups located at the sepiolite surface, appearing at approximately 3720 cm^{-1} in the starting silicate, disappear in the TiO_2−sepiolite nanocomposites. It is known that the coverage by CTA^+ species perturbs this band,[37] but this band is again observed as a shoulder after calcination when the organic matter has been removed. The lack of such an IR band in the TiO_2−sepiolite materials indicates, in agreement with the TEM and FE-SEM images, the almost complete coverage of the sepiolite surface by the metal−oxide nanoparticles that probably are grafted to the silicate through Si−O−Ti bridges, contributing in this manner to the stability of the nanocomposites (Figure 4). In this way, it can be assumed that the reaction of the highly reactive silanol groups at the surface of the sepiolite with the titanium alkoxides may lead, in a first step, to a thin oxide layer from which the TiO_2 nanoparticles can grow further. However, the relatively reduced number of Si−O−Ti bonds located at the sepiolite−titania interphase and the overlapping of the associated IR absorption bands with the intense pattern of the mineral prevent the observation of such vibration bands in the corresponding IR spectra for definite confirmation of grafting.

On the basis of the procedure for the preparation of S-doped TiO_2−sepiolite nanocomposites, we have prepared silica–titania mixed oxides on the sepiolite surface. It is expected that the incorporation of silica could contribute to the development of a higher surface area in the resulting solids and at the same time may improve the anchorage to the external silanol groups of sepiolite through siloxane bonds. In this case, mixtures of TMOS and TIPOTI as starting reagents acting as silica and titania sources, respectively, were used with 2:6:1 and 6:4:5 (CTA−sepiolite/TIPOTI/TMOS) as the weight ratios of the components. Applying these ratios, the final total oxides content (i.e., TiO_2 and SiO_2) after calcination were expected to be 40% TiO_2, 10% SiO_2 and 10% TiO_2, 40% SiO_2, respectively. These samples were also S-doped by incorporation of thiourea to the starting mixture of reagents. The effect on the surface area increase of the incorporation of SiO_2 is clearly observed by comparing the 2:6:1 and 6:4:5 (CTA−sepiolite/TIPOTI/TMOS) weight ratio values for the samples (Table 2). However, it is found that the presence of silica influences the amount of carbon content in the final sample that increases with the silica content in the sample. At the same time, the sulfur content decreases, as only TiO_2 nanoparticles are responsible of the S-doping. The samples containing only S-doped TiO_2 show the sulfur content to be in the 1.3% to 1.8% range (Table 1). It should be noted that the presence of carbon and sulfur in the resulting nanocomposites could affect the surface properties of the resulting materials, such as their photocatalytic activity.

The different TiO_2−sepiolite nanocomposites reported here are materials that combine different characteristics that could be of interest from the point of view of their surface properties. In this sense, the photocatalytic activity of several samples stabilizing anatase (S-doped) was tested in batch experiments involving phenol as a pollutant model molecule.

Table 2. Textural Properties Deduced from the N_2 BET Isotherms Determined in Various TiO_2−Sepiolite Derivatives Prepared in This Work

sample starting composition	calcination conditions	S_{BET} ($m^2 \cdot g^{-1}$)	S_{ext} ($m^2 \cdot g^{-1}$)	V_t ($cm^3 \cdot g^{-1}$)	V_{mic} ($cm^3 \cdot g^{-1}$)
CTA−sepiolite	uncalcined	90	90	0.317	0
	500 °C, 1 h N_2, 5 h air	194	152	0.383	0.018
CTA−sepiolite/TIPOTI 1:1	500 °C, 1 h N_2, 5 h air	169	146	0.221	0.010
CTA−sepiolite/TIPOTI 1:2	500 °C, 1 h N_2, 5 h air	155	144	0.214	0.006
CTA−sepiolite/thiourea−TIPOTI[a] 1:2	500 °C, 6 h air	161	122	0.198	0.016
CTA−sepiolite/thiourea−TIPOTI[a] 1:3	uncalcined	35	25	0.049	0.004
	500 °C, 4 h air	111	91	0.142	0.008
	500 °C, 6 h air	124	98	0.147	0.011
	550 °C, 6 h air	83	49	0.109	0.014
	600 °C, 4 h air	79	60	0.124	0.008
CTA−sepiolite/thiourea−TIPOTI[a] 1:4	500 °C, 6 h air	163	137	0.180	0.011
CTA−sepiolite/thiourea−TIPOTI[a]/TMOS 2:6:1	500 °C, 6 h air	136	136	0.149	0.000
CTA−sepiolite/thiourea−TIPOTI[a]/TMOS 6:4:5	500 °C, 6 h air	263	154	0.356	0.050

[a] Reaction mixture incorporating a 4:1 thiourea/TIPOTI ratio.

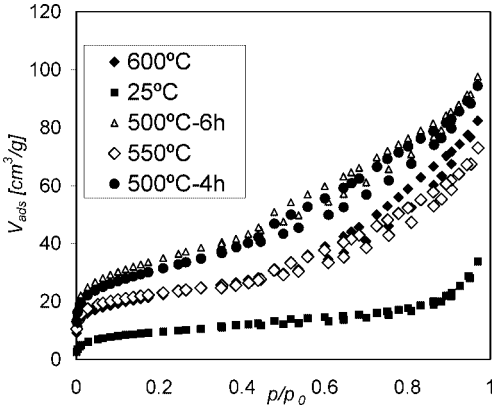

Figure 6. N_2 adsorption isotherms obtained for the S-doped TiO_2−sepiolite nanocomposites (samples from CTA−sepiolite/thiourea−TIPOTI 1:3 ratio) uncalcined and calcined at 500, 550, and 600 °C.

As indicated in the experimental section, the experiments were carried out using a thermostatic photoreactor (see Figure 1S in the Supporting Information) with a total irradiation time of 2 h. The changes in the organic pollutant content during the irradiation were determined from the carbon content of the system that was monitored by TOC measurement shown in Figure 8. In this figure, the high efficiency of S-doped TiO_2−sepiolite nanocomposites is observed, showing the maximum photodegradation rate which is almost complete after 2 h of irradiation. These results are in good agreement with recent results of S-doped TiO_2 prepared by sol–gel procedures, showing the improvement of the S-doping in the photocatalytic activity.[57] The activity of these samples increases with the TiO_2 content in the nanocomposites (i.e., 1:2 and 1:3 clay/TIPOTI-S samples) in which 82 and 92% of the organic matter was photodegraded, respectively (see Table S1 in the Supporting Information). The higher activity of these samples is significant compared to that of the starting sepiolite and S-doped anatase prepared from the xerogel generated by TIPOTI hydrolysis, separately. A positive synergistic effect in the photocatalytic activity of the TiO_2−clay systems has been also reported in titania-layered clay minerals (e.g., Na−montmorillonite) using dichloroacetic acid in similar photodegradation experi-

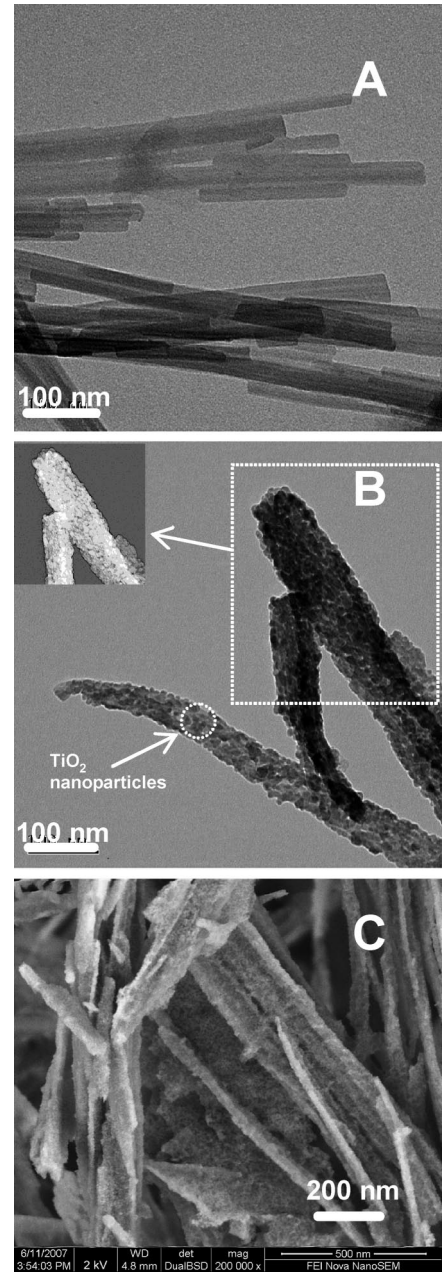

Figure 7. TEM images of starting CTA−sepiolite microfibers (A) and S-doped TiO_2/sepiolite nanocomposite (sample calcined at 500 °C for 4 h in air, B) and an FE-SEM image of sample B (C). The inset in B represents the negative picture to remark the presence of nanoparticles covering the sepiolite fiber.

(57) Crisan, M.; Braileanu, A.; Raileanu, M.; Crisan, D.; Dragan, N.; Anastasescu, M.; Galtayries, A.; Ianculescu, A.; Gravila, R.; Nitoi, I.; Oancea, P. *XIV International Sol-Gel Conference Abstracts*; ENSCM Communication: Montpellier, France, 2007; p 465.

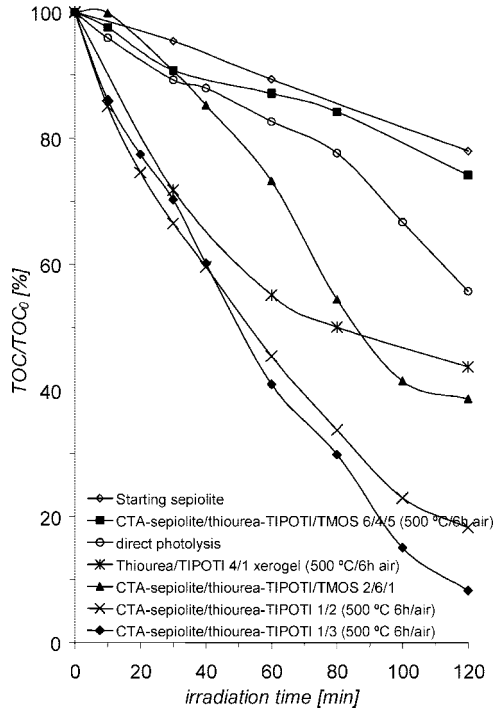

Figure 8. Curves of photocatalytic activity (deduced from TOC results) of different TiO_2−sepiolite nanocomposites in the photodegradation reaction of phenol.

ments.[13] In our case, this feature can be related to the high specific surface area of TiO_2 nanoparticles homogeneously distributed on the sepiolite surface (Table 2). However, the nanocomposites containing SiO_2 and TiO_2 that show a higher specific surface area do not present a higher activity because of the presence of the silica–titania mixed oxides in place of the anatase. Moreover, the photoactivity of samples with high silica content is even lower than that of direct photolysis. This feature can be related to a protection of the phenol molecules by their adsorption on the inorganic support which produces a shielding effect. The starting sepiolite shows a similar behavior (Figure 8).

4. Concluding Remarks

Inorganic–inorganic nanocomposites containing stabilized TiO_2 anatase nanoparticles on the surface of sepiolite have been prepared following a colloidal route involving the use of a cationic surfactant that modifies the external surface of the silicate. This modification confers organophilic properties to the sepiolite microfibers allowing the incorporation of alkoxides (TIPOTI and TMOS) that can be further hydrolyzed in a controlled manner. The resulting intermediate materials give TiO_2−sepiolite nanocomposites in the form of nanoparticles that are generated on the silicate surface after thermal treatments to remove the organic matter and to crystallize the titanium oxide. The effect of the nature of the surfactant may influence the morphology (size and shape) of the TiO_2 nanoparticles which must be studied in depth. The incorporation of thiourea to the initial colloidal system stabilizes the anatase phase because of the sulfur atoms incorporated into the titanium dioxide crystal lattice during the thermal treatment. Optimization of the experimental conditions and, particularly, the thermal treatment allows the preparation of nanocomposites that show maximum specific surface area and porosity, incorporating 4–8 nm TiO_2 anatase nanoparticles on the external surface of the pristine sepiolite fibers.

Preliminary tests on the photocatalytic activity of the TiO_2−sepiolite nanocomposites show high efficiency in the phenol degradation that can reach more than 90% of conversion. The microfibrous nanocomposite materials are most efficient as photocatalyst systems with the clay sample and the anatase nanoparticles acting separately, showing in this way a synergistic effect that will be more deeply discussed in a publication elsewhere.

Supporting Information Available: This material includes additional figures of the photoreactor used for the photocatalysis tests, XRD patterns of the calcined, both undoped and S-doped, TiO_2 xerogels, and additional FE-SEM and TEM images of the different sepiolite derivatives, as well as a table with data on the variation of the TOC at different times of the photodegradation reaction (PDF). This material is available free of charge via the Internet at http://pubs.acs.org.

Acknowledgment. This work has been promoted by the CSIC and the Hungarian Academy of Sciences (Bilateral Project 2004HU0021), and it has been partially supported by the CICYT, Spain (Projects: MAT2003-06003-C02-01, BTE2003-05757-C02-02, and MAT2006-03356), and the Péter Pázmány Program of the Hungarian National Office of Research and Technology (No. RET-07/2005). We thank Mr. F. Pinto and Ms. S. Paniagua for technical assistance in TEM, SEM, and EDAX studies and Mr. T. García-Somolinos for his help in the surface area determinations.

CM702251F